Photothermal Electrical Resonance Spectroscopy of Physisorbed Molecules on a Nanowire Resonator

ARTICLE *in* NANO LETTERS · JULY 2015

Impact Factor: 13.59

3 AUTHORS:

K. Prashanthi

University of Alberta

47 PUBLICATIONS **224** CITATIONS

SEE PROFILE

Arindam Phani

University of Alberta

10 PUBLICATIONS **9** CITATIONS

SEE PROFILE

Thomas Thundat

University of Alberta

476 PUBLICATIONS **11,585** CITATIONS

SEE PROFILE

NANO LETTERS

Letter

pubs.acs.org/NanoLett

Photothermal Electrical Resonance Spectroscopy of Physisorbed Molecules on a Nanowire Resonator

Kovur Prashanthi,* Arindam Phani, and Thomas Thundat*

Department of Chemical and Materials Engineering, University of Alberta, Edmonton AB T6G 2R3, Canada

Supporting Information

ABSTRACT: Mid-infrared (IR) photothermal spectroscopy of adsorbed molecules is an ideal technique for molecular recognition in miniature sensors with very small thermal mass. Here, we report on combining the photothermal spectroscopy with electrical resonance of a semiconductor nanowire for enhanced sensitivity, selectivity, and simplified readout. Wide band gap semiconductor bismuth ferrite nanowire, by virtue of its very low thermal mass and abundance of surface states in the band gap, facilitates thermally induced charge carrier trapping in the surface states, which affects its electrical resonance response. Electrical resonance response of the nanowire varies significantly depending on the photothermal spectrum of the adsorbed molecules. We demonstrate highly selective detection of mid-IR photothermal spectral signatures of femtogram level molecules physisorbed on a nanowire by monitoring internal dissipation response at its electrical resonance.

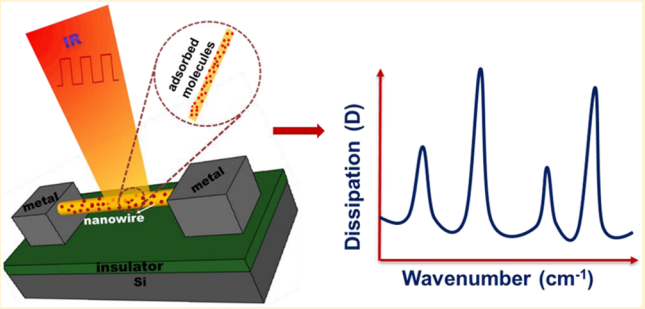

KEYWORDS: *Nanowire sensors, nanowire resonators, photothermal spectroscopy, infrared sensor, molecular recognition, temperature-induced dissipation in nanowires*

Nanosensor platforms such as nanowires[1−5] and nanocantilevers[6,7] are topics of active research because of their potential as a miniature sensor platform with unprecedented sensitivity for applications ranging from health-care to national security. In general, molecular adsorption-induced changes in nanosensor physical properties serve as the sensor signal. Imparting chemical selectivity for small molecule detection to these sensor systems for reversible detection has been a challenge. Commonly used method of using immobilized chemoselective coatings often results in high false positives due to the generic nature of reversible chemical interactions. Hence, developing concepts that do not require immobilized chemical interfaces are very attractive. One such technique that exploits the very high thermal sensitivity of a bimaterial microcantilever is photothermal cantilever deflection spectroscopy where IR excitation of adsorbed molecules and the subsequent nonradiative decay results in mechanical bending of the cantilever.[8−10] Nanomechanical deflection of the cantilever as a function of excitation wavelength shows the molecular vibrational characteristics of the adsorbates.[9,10] This nanomechanical spectrum is complementary to that obtained with conventional IR spectroscopies such as FTIR. Thermomechanical detection of spectroscopic signals does not rely on Beer−Lambert principle, and, therefore, the relative intensities of the peaks are complementary to that of conventional IR spectra. However, the locations of the peaks (energy, $h\nu$) match very well with that of conventional spectroscopies, making nanomechanical spectroscopy highly selective and sensitive. Another advantage of the technique is that it works for physisorbed molecules, making sensor regeneration at room temperature easy.[9,10,8]

The sensitivity of detection in the nanomechanical spectroscopic technique depends on the thermal mass of the sensor. Therefore, lowering the thermal mass of the detector could result in superior sensitivity in chemical sensing. Because a nanowire has a very small thermal mass, it can be an ideal sensor for photothermal spectroscopy. However, measuring nanomechanical bending of a nanowire caused by bimaterial effect is very challenging using optical readout techniques. In general, monitoring nanomechanical motion of nanostructures such as nanoribbons and nanocantilevers, induced by small temperature changes, requires complex and bulky equipment.[7,11−13]

In this Letter, we introduce a method of combining photothermal spectroscopy of physisorbed molecules on a semiconductor nanowire with its electrical resonance response for unprecedented selectivity and sensitivity. This technique, therefore, combines the selectivity of mid-IR spectroscopy and sensitivity offered by electrical resonance phenomenon. Wide band gap materials such as bismuth ferrite ($BiFeO_3$ or BFO) have high density of surface states in their band gap, which are filled up to the Fermi level.[14−16] Because of the high surface-to-volume ratio of a BFO nanowire, its electrical properties are significantly influenced by the electrical nature of the surface

Received: June 28, 2015
Revised: July 25, 2015
Published: July 28, 2015

DOI: 10.1021/acs.nanolett.5b02557
Nano Lett. 2015, 15, 5658−5663

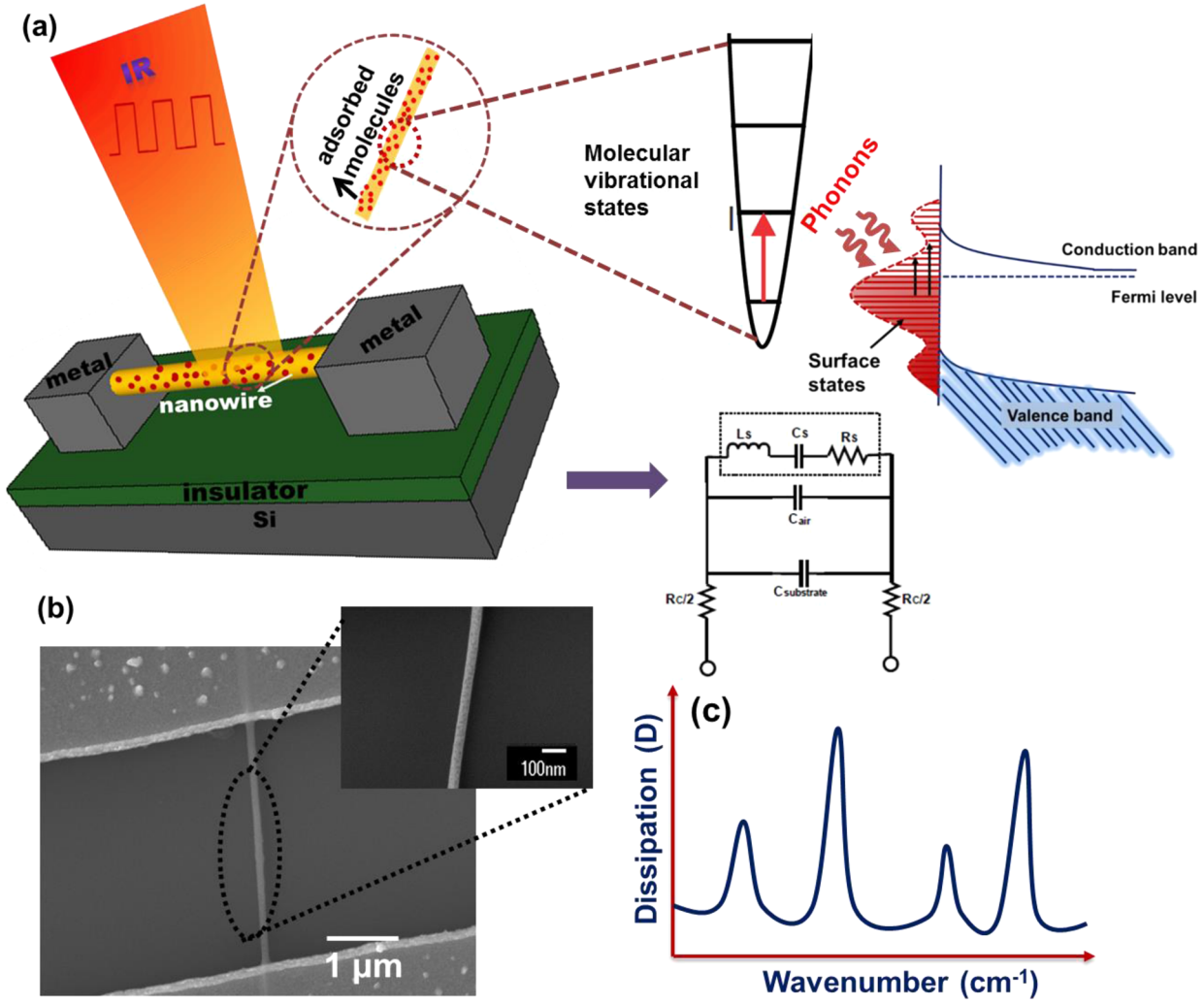

Figure 1. (a) Schematic representation nanowire resonator with equivalent electrical circuit model (please refer to section 1a, Supporting Information) and the concept of coupling electrical resonances of the nanowire with optical excitation for high selectivity and high sensitivity chemical sensing, (b) SEM images of BFO nanowire, (c) dissipation (D) IR spectrum of adsorbed molecules. Electrical resonance frequency of the nanowire changes due to molecular adsorption, enabling detection of fg levels of adsorbed mass. Resonant IR excitation of adsorbed molecules produce large changes in the dissipation of nanowire resonator due to population−depopulation of surface states by thermally generated carriers.

states.[17,16] Changing the temperature of the nanowire modulates the occupation of these surface states. Because the thermal mass of a nanowire is extremely small, absorption of very small quantities of heat can result in large changes in its temperature and in turn cause changes in the carrier population/depopulation of the surface states. Alternatively, small internal changes in heat from phonon excitations can effect similar repartitioning of surface states. This fact can be used to an advantage where, by illuminating the nanowire with pulsed light, we show this can modulate the population-depopulation of these surface states depending on excitation and relaxation of molecular vibrations of the adsorbed molecules. A slight variation in temperature from nonradiative relaxation induces changes in the surface state population further changing the electrical properties of the nanowire, which can be detected by monitoring the electrical resonance response of the nanowire.

A schematic of our photothermal electrical resonance spectroscopy (PERS) technique is illustrated in Figure 1. A suspended BFO nanowire (3−20 μm in length with a radius of 100 nm) electrically connected to metal (Pt/Ti) electrodes forms the electrical nanowire resonator (Figure 1a). A scanning electron microscopy (SEM) image of BFO nanowire is shown in Figure 1b. Any change in the electrical properties of the nanowire changes the electrical resonance frequency of the circuit. The electrical resonance frequency of a nanowire also changes due to molecular adsorption (capacitive loading) as well as from changes in temperature due to optical excitation of the adsorbed molecules (surface state population-depopulation). However, these changes in the electrical resonance frequency are too small for high sensitivity detection. We have realized that though the changes in resonance frequency are small, the resonance response of dissipation is extremely sensitive to changes in temperature changes. Only dissipation shows significant variations due to IR excitation of adsorbed molecules on the nanowire resonator. We record these dissipation signatures at electrical resonance of nanowire as a function of incident mid-IR wavelengths, and they correspond to a dissipation spectrum (photothermal electrical resonance spectrum or PERS) unique to excited vibrational states of physisorbed molecules (Figure 1c).

DOI: 10.1021/acs.nanolett.5b02557
Nano Lett. 2015, 15, 5658−5663

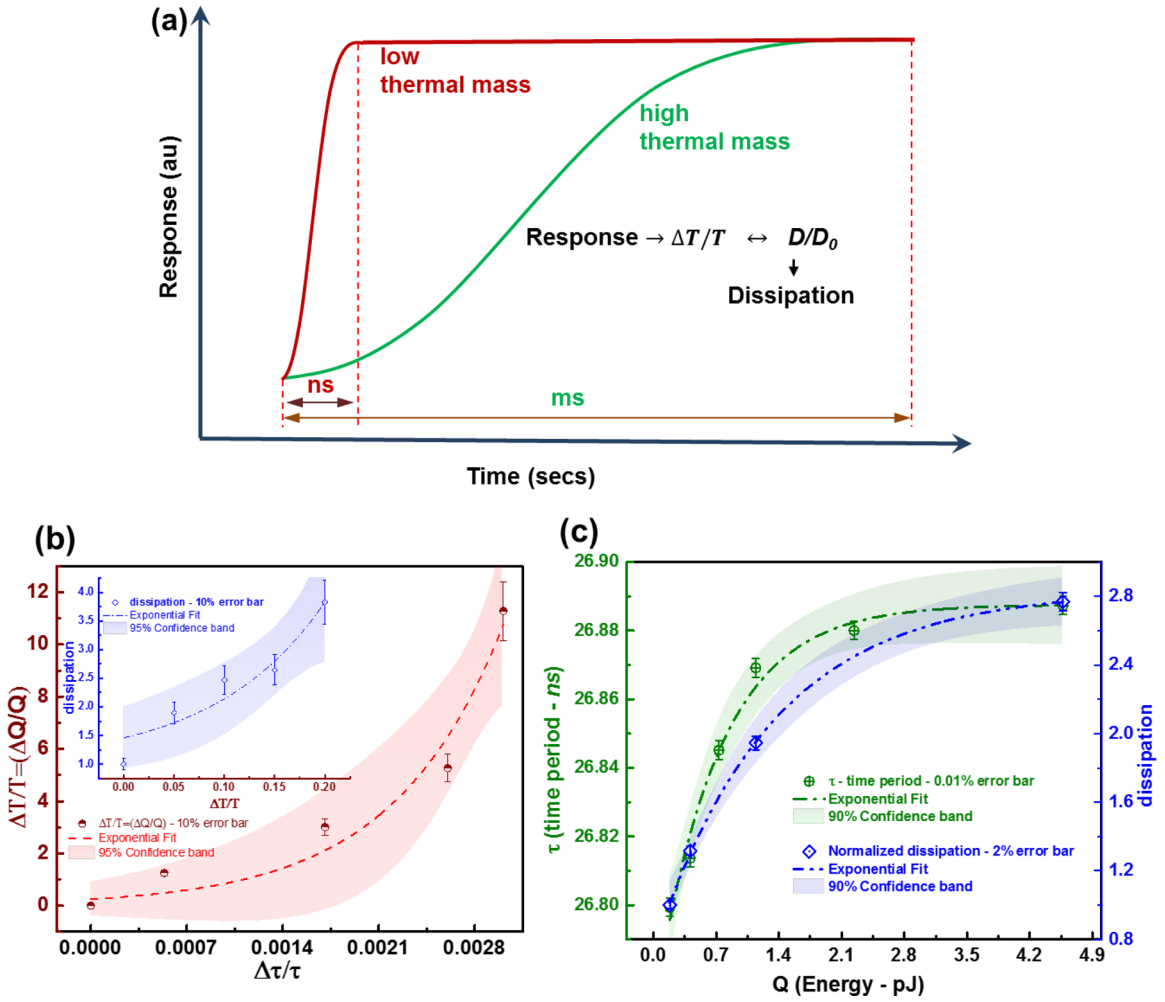

Figure 2. (a) Typical time response curve for low thermal mass and high thermal mass systems. (b) Thermal response sensitivity of nanowire resonator with low thermal mass analyzed at SRF as a function of external drive. Inset shows normalized changes in dissipation (D/D_0) as a function of relative changes above room temperature. (c) Time response (τ) variations as a function of heat energy (Q) floor corresponding to external drive; subsequent variations in normalized dissipation (D/D_0) of the nanowire resonator for the same energy fluctuations. Electronic state distribution in a material typically follows Boltzmann distribution and hence their variations as a function of energy all follow logarithmic trends, evident from thermal responses.

A nanowire behaves analogous to an electrical series *RLC* resonant circuit (Figure 1a) with effective inductance L and a nonideal capacitance C, showing resonance frequency $f_{res} = 1/(2\pi(LC)^{1/2})$ in the megahertz regime as measured (see Supporting Information Section 1). The corresponding response time scale, $\tau = 1/f_{res}$ (tens of nanoseconds, ns) as obtained from the resonance analysis, essentially becomes the time scale of changes in electrical characteristics due to increased thermal energy of ΔQ arising from phonon-assisted transitions. Cantilever-based photothermal sensors, having higher thermal mass, are typically slow (milliseconds, ms) and they fail to track ΔT at a fast enough time scale (ns). Electrical resonance of nanowires makes that fast tracking (ns) possible and has the effect of enhancing the detection of heat changes arising from phonon-transitions internally. The very low thermal mass of the suspended nanowire effectively results in a high rate of change in temperature $(\partial T/\partial \tau)\uparrow$ as a function of time. In essence, the energy from any phonon relaxation gets dissipated internally and it is possible to monitor the dynamic dissipation at the resonance as a ratio of energy dissipated to energy of excitation per cycle. This dimensionless quantity known as dissipation (in electrical terms it called *D*-factor) can be measured for different IR incident wavelengths. The dissipation (or *D*-factor) has been used earlier as a sensor signal for differential detection of volatile chemicals[18,19] A detailed discussion on the electrical definition of *D*-factor is presented in Supporting Information Section 1.

Absorption of IR energy resonantly excites vibrational states of molecules physisorbed on the nanowire. Nonradiative decay of these excited states cause thermal changes through multiphonon relaxation processes. Such phonon-induced changes in heat ΔQ depend on the thermal-mass mC_P (m being the mass and C_P the thermal heat capacity) and result in a measurable temperature change $\Delta T = \Delta Q/mC_P$, scaling inversely with the detector thermal mass. In all conventional forms of detection, measurable ΔT relies on the change in electrical property arising from this ΔQ. Inherent limitations on time scale responses thus poses a fundamental limit to the detection sensitivity of ΔQ over thermal noise originating from any such phonon interaction process. At bulk scales, the overall response time is long and it demands a high ΔQ or multiple nonradiative relaxations integrated over time to produce a steady state electrical property change. However, in a very low thermal mass nanosystems like nanowire, thermal changes can

DOI: 10.1021/acs.nanolett.5b02557
Nano Lett. 2015, 15, 5658−5663

be significant and at a very small time scale. An electrical property change in a semiconductor nanowire is predominantly brought about by the distribution of carriers in its electronic states. A change in ΔQ which can bring about a change in the carrier distribution by populating vacant higher electronic states with thermally induced carriers, would change its electrical property.

The importance of surface-states in modulating responses of bulk semiconductor materials through surface charges was addressed in the early 1970s by Lagowski and Gatos.[20,21] Catalan's review reveals prospects on similar grounds in semiconductor BFO.[22] Phonon de-excitations are usually in the form of a cascading multiphonon assisted relaxation process reflected as internal dissipation[23−25] and is attributed to phonon−phonon interactions or scattering. Defects in bulk or on the surface enhances it significantly[26−28] and they play a crucial role at the nanoscale as in our method. For a system with high surface state density, there is a higher probability of coupling phonon relaxation energy $(\Delta Q)_{\text{phonon}}$ in promoting a charge carrier to an allowable vacant surface states above the Fermi level; traditionally termed charge capture or carrier trapping,[26−28] which we exploit to our advantage by monitoring through electrical resonance. In the electrical domain, such carrier repartitioning into different allowable surface states reflect a dominant capacitive reactance (X_C) change, as shown in our experiments. The electrical parameter definitions are given in Supporting Information Section 1.

Higher thermal mass sensors have slow response time (~ms) as compared to low thermal mass systems as illustrated in Figure 2a and hence their usual steady state electrical property change used as a measurement signal, fails to track ΔT at a fast enough time scale. The dependence of external excitation energy $\Delta Q = (i^2 R_S/f_{res})$ (R_S being the equivalent series resistance) on f_{res}, gives the relative thermal sensitivity $\Delta T/T = \Delta Q/Q$ of the nanowire electrical resonance as a function of relative time scale response $\Delta\tau/\tau$ at electrical resonance, showing an enhanced exponential sensitivity (Figure 2b), where $\tau = 1/f_{res}$. Such an increased sensitivity at time scales of the order of tens of ns in energy space, as evident more in Figure 2c makes sensitive discrimination of ΔQ possible even at normal conditions. Since the thermal-mass of the nanowire resonator is negligible, ΔT can be significantly greater than the thermal noise. The measured normalized dissipation (D/D_0) in Figure 2b (inset) and 2c shows the temperature-induced effective changes in internal losses at the same time scale. The nanowire thus serves as an extremely sensitive thermal sensor and an electrical resonator platform, enabling recognition of adsorbed molecules through monitored variations in its dynamic impedance parameters.

To demonstrate the capabilities of the sensor platform, we have chosen commonly investigated explosive, cyclotrimethylene trinitramine (RDX) as model system. Because these explosive molecules bind to surfaces very easily, they remain on the nanowires for longer periods enabling repeated measurements. The changes in resonance frequency of a nanowire due to the adsorption of RDX are presented in Figure 3. As mentioned earlier, both resonance frequency and dissipation vary as a function of molecular adsorption due to mass loading (inset of Figure 3). A detailed analysis of experimental data on other set of nanowire resonators with similar trend has been presented in Supporting Information Section 2. The higher surface area of a nanowire coupled with higher number of surface states promotes unprecedented mass resolution in

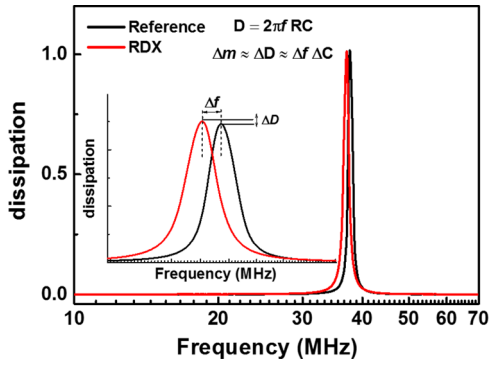

Figure 3. Electrical resonance of the nanowire resonator without and with adsorbed RDX molecules. The dissipation of the nanowire resonator also changes as a function of molecular adsorption. Inset of shows higher magnification in the region of interest.

detection. Adsorbed mass on the nanowire resonator from the resonance response shift and corresponding capacitance change is calculated as a function of charge donation or transfer from the adsorbed chemical species[29] of unknown mass and is estimated to be of the order of 10 fg. This estimated mass is also verified within the same order of magnitude (60 fg), assuming fractional two-dimensional (2D) surface exposure of the nanowire to 0.4 μL droplet (used in experiment). The factor of variation between the measured capacitance change and the surface area exposure estimation may be accounted for the nonuniform and different evaporation kinetics of solvent on the surface of the nanowire and the substrate (see Supporting Information Section 3). It is possible that RDX adsorption on the nanowire cannot be in the form of a continuous layer, instead would be in the form of discrete islands on the nanowire surface and hence monolayer assumption would tend to overestimate the adsorbed mass. The technique thus also opens up a novel way of estimating adsorbed mass from electrical property variation through dynamic dissipation study at resonance.

The variation in the amplitude of dissipation corresponding to IR absorption wavenumbers of RDX is shown in Figure 4a. The normalized dissipation, D/D_0 (corresponding to each IR wavenumber) as a function of relative time scale response, $\Delta\tau/\tau$ (Figure 4b) reveals an exponential nature of thermal response, where the change is from excited thermal phonons, which couple to the surface states of the nanowire through multiphonon assisted relaxation processes. The higher dissipation as a function of IR is from phonon induced ΔT analogous to more effective internal dissipation as clear from Figure 2. In essence, the thermally induced carrier repartitioning within the surface states change the way energy from external electrical drive gets dissipated and stored in the nanowire resonator per cycle of its oscillation at resonance. This resonance response variation, typical of the nanowire system employed, provides deeper insights on the thermal response characteristics (please refer to Figure 2), which is exploited here as a basis for our unique way of receptor free IR chemical discrimination. In electrical terms, the variations in the dissipation are from the changes in the effective capacitance of the nanowire. An increasing capacitance decreases the capacitive reactance, X_C (see Supporting Information Section 4) and thus stores less energy per cycle. Effectively the internal dissipation of nanowire increases showing higher D-factor. The variation in the capacitive reactance, affecting the nanowire

DOI: 10.1021/acs.nanolett.5b02557
Nano Lett. 2015, 15, 5658−5663

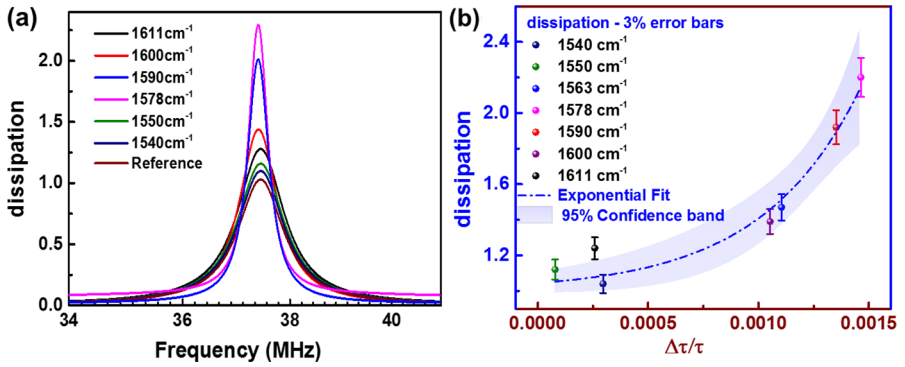

Figure 4. (a) Dynamic dissipation of the nanowire resonator with RDX molecules adsorbed on its surface and irradiated by IR. (b) Normalized dissipation (D/D_0) response of the nanowire resonator as a function of its response time. The selectivity in detection is through to the unique spectral absorption characteristics of the adsorbates in the mid-IR region. A variation in internal dissipation of the nanowire resonator is reflected by its dynamic dissipation in proportion to the small temperature changes due to IR absorption by adsorbates. The dynamic dissipation of the nanowire resonator with adsorbed molecules (without IR irradiation) served as the reference signal.

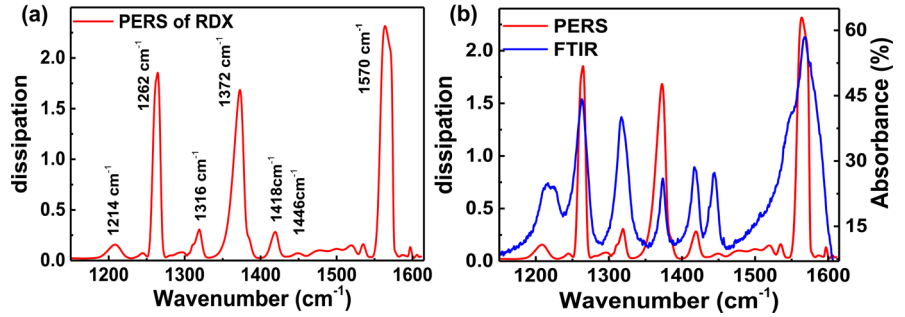

Figure 5. (a) PERS of RDX molecules adsorbed on nanowire and (b) comparison PERS and FTIR spectroscopy of RDX molecules. The peaks on the measured PERS matches very well with the FTIR spectra of the analyte molecules. The observed high spectral resolution (line width) in PERS of the nanowire resonator is due to its extremely low thermal mass and fast response time ns significantly reducing thermal broadening compared to FTIR. FTIR absorbance ≈ photon count; dissipation from IR absorption is a complementary response in terms of phonon-induced heat.

response, reflects the variations in the charge state of surface energy levels of the semiconductor nanowire. It is believed that the observed increase in surface capacitance is a result of an increase in surface charge carriers (electrons or holes) in the unoccupied surface states of the BFO nanowire by multi-phonon process and has been reported previously for metal-oxide-semiconductor (MOS) thin films.[23,24]

A systematic recording of the variations in dissipation as a function of incident IR wavelengths gives the spectrum of the adsorbed species, bringing selectivity. Experimentally observed spectrum of RDX molecules adsorbed on nanowire is presented in Figure 5a. Dissipation spectra as a function of IR wavelengths for the nanowire without the adsorbed analyte molecules becomes the reference or background signal in our analysis and is used for background corrections. Figure 5b shows comparison of PERS and FTIR spectra. The observed peaks in the dissipation signature match the FTIR spectra peak positions, showing selectivity and sensitivity of this approach. The line-widths of the dissipation spectrum are much sharper and are primarily due to the low thermal mass and high electrical resonance frequency of the nanowire. Usually, the broadening of the peaks in conventional solid and liquid phase IR spectra is caused by the relaxation and dephasing of the vibrational excited states and indicates the complex fast dynamic interaction of the molecule with its environment. The high inherent nanowire resonance frequency along with the low thermal mass has the advantage of faster dynamic response as evident from discussions and results (Figure 2) and is reflected in the obtained spectra as unique sharp peaks with a significant low line width broadening compared to FTIR spectra (Figure 5b).

In conclusion, combining electrical resonance of a BFO nanowire with mid-IR photothermal effect allows molecular recognition of femtogram (fg) levels of physisorbed molecules on a single BFO nanowire. IR excitation of the physisorbed molecules increases the temperature of the nanowire due to its low thermal mass. Because of the presence of high density of surface states on the nanowire, changes in temperature promotes carrier trapping that in turn changes the electrical resonance parameters of the nanowire. The BFO nanowire system described here utilizes the internal dissipation due to IR absorption by the adsorbed molecules and opens new opportunities for detecting minute amounts of surface adsorbed molecules on similar nanomechanical resonating platforms using dissipation as the parameter. With optimization, this method provides exciting opportunities in developing a sensitive platform with superior selectivity performance.

Materials and Methods. *Preparation of BFO Nanowire Resonator.* BFO nanowire resonators with various electrode spacing are fabricated directly on prepatterned substrates by electrospinning technique as reported in our previous work.[17] A gas injection system available with motorized flexible *xyz*-drive was used for in situ platinum metal contact to these nanowires (RAITH150). The residues of explosive molecules of RDX was deposited on the nanowire resonator using the droplet evaporation method.

DOI: 10.1021/acs.nanolett.5b02557
Nano Lett. 2015, 15, 5658−5663

Chemicals. The standard explosive RDX samples were purchased from AccuStandard, Inc. (New Haven, CT) and used without further purification. The standard concentration of each explosive is 1000 μg/mL in MeOH/ACCN (1:1) as indicated by the manufacturer.

Photothermal Electrical Resonance Spectroscopy Setup. The IR radiation (pulsed at 200 kHz) from the quantum cascade laser (Daylight Solutions UT-8) was focused on the nanowire resonator. The laser peak power was in the range of 100−800 mW depending on the wavelength of operation. For UT-8, the peak power was 400 mW at 8.2 μm wavelength. The specified average power for this laser was up to 20 mW. The wavenumber of IR source was fixed at a specific value (range: 1630−1150 cm^{-1}) and the corresponding dissipation parameters were measured. The impedance parameters of the nanowire resonator were measured using an Agilent 4294A impedance analyzer having a frequency range of 40 Hz to 110 MHz with nominal impedance accuracy: ±0.08% at 100 Hz. The excellent high quality factor (Q) or D accuracy enables reliable analysis of low-loss components. The inherent high dynamic range of the equipment allows evaluation under actual operating conditions. A fixed ac test signal level $V_{rms} \sim 50$ mV was employed as input drive voltage for all the impedance measurements.

FTIR Spectroscopy. The explosive residues were characterized using a standard FTIR Thermo Scientific Nicolet Contihuμm infrared microscope with a potassium bromide beam splitter and a MCT-A (narrow band 650 cm^{-1} cutoff) detector microscope in reflection mode. The number of registered scans was 200 with resolution of 4 cm^{-1}.

■ ASSOCIATED CONTENT

Supporting Information

The Supporting Information is available free of charge on the ACS Publications website at DOI: 10.1021/acs.nanolett.5b02557.

Additional details on the electrical resonance of nanowire resonators, definitions of the electrical parameters, a detailed analysis of experimental data on another set of nanowire resonators, and calculations of adsorbed mass on nanowire using electrical resonance. (PDF)

■ AUTHOR INFORMATION

Corresponding Authors

*E-mail: kovur@ualberta.ca.
*E-mail: thundat@ualberta.ca.

Notes

The authors declare no competing financial interest.

■ ACKNOWLEDGMENTS

This work was supported by Canada Excellence Research Chairs Program. The authors would like to acknowledge X. Liu in helping with IR setup and J. E. Hawk for developing automated data acquistion software which was used to collect the data.

■ REFERENCES

(1) McAlpine, M. C.; Ahmad, H.; Wang, D.; Heath, J. R. *Nat. Mater.* **2007**, *6* (5), 379−384.
(2) Penner, R. M. *Annu. Rev. Anal. Chem.* **2012**, *5*, 461−485.
(3) Liu, H.; Kameoka, J.; Czaplewski, D. A.; Craighead, H. G. *Nano Lett.* **2004**, *4* (4), 671−675.
(4) Patolsky, F.; Lieber, C. M. *Mater. Today* **2005**, *8*, 20−28.
(5) Lieber, C. M. *MRS Bull.* **2011**, *36* (12), 1052−1063.
(6) Yang, Y. T.; Callegari, C.; Feng, X. L.; Ekinci, K. L.; Roukes, M. L. *Nano Lett.* **2006**, *6* (4), 583−586.
(7) Li, M.; Tang, H. X.; Roukes, M. L. *Nat. Nanotechnol.* **2007**, *2* (2), 114−120.
(8) Krause, A. R.; Van Neste, C.; Senesac, L.; Thundat, T.; Finot, E. *J. Appl. Phys.* **2008**, *103* (9), 094906.
(9) Kim, S.; Lee, D.; Liu, X.; Van Neste, C.; Jeon, S.; Thundat, T. *Sci. Rep.* **2013**, *3*, 1111.
(10) Bagheri, M.; Chae, I.; Lee, D.; Kim, S.; Thundat, T. *Sens. Actuators, B* **2014**, *191*, 765−769.
(11) Zhang, X. C.; Myers, E. B.; Sader, J. E.; Roukes, M. L. *Nano Lett.* **2013**, *13* (4), 1528−1534.
(12) McCaig, H. C.; Myers, E.; Lewis, N. S.; Roukes, M. L. *Nano Lett.* **2014**, *14* (7), 3728−3732.
(13) Hanay, M. S.; Kelber, S.; Naik, a K.; Chi, D.; Hentz, S.; Bullard, E. C.; Colinet, E.; Duraffourg, L.; Roukes, M. L. *Nat. Nanotechnol.* **2012**, *7* (9), 602−608.
(14) Prashanthi, K.; Thakur, G.; Thundat, T. *Surf. Sci.* **2012**, *606* (19−20), L83−L86.
(15) Prashanthi, K.; Thundat, T. *Scanning* **2013**, *36*, 224−230.
(16) Prashanthi, K.; Dhandharia, P.; Miriyala, N.; Gaikwad, R.; Barlage, D.; Thundat, T. *Nano Energy* **2015**, *13*, 240−248.
(17) Prashanthi, K.; Gaikwad, R.; Thundat, T. *Nanotechnology* **2013**, *24* (50), 505710.
(18) Weimar, U.; Göpel, W. *Sens. Actuators, B* **1998**, *52* (1−2), 143−161.
(19) Amrani, M. E. H.; Persaud, K. C.; Payne, P. A. *Meas. Sci. Technol.* **1995**, *6* (10), 1500−1507.
(20) Lagowski, J.; Balestra, C. L.; Gatos, H. C. *Surf. Sci.* **1972**, *29*, 213−229.
(21) Gatos, H. C. *J. Vac. Sci. Technol.* **1973**, *10* (1), 130.
(22) Catalan, G.; Scott, J. F. *Adv. Mater.* **2009**, *21* (24), 2463−2485.
(23) Garetto, D.; Randriamihaja, Y. *IEEE Trans. Electron Devices* **2012**, *59* (3), 610−620.
(24) Garetto, D.; Randriamihaja, Y. M.; Zaka, A.; Rideau, D.; Schmid, A.; Jaouen, H.; Leblebici, Y. *Solid-State Electron.* **2012**, *71*, 74−79.
(25) Garetto, D.; Randriamihaja, Y. *IEEE Trans. Electron Devices* **2012**, *59* (3), 621−630.
(26) Henry, C. H.; Lang, D. V. *Phys. Rev. B* **1977**, *15*, 989−1016.
(27) Burt, M. *J. Phys. C: Solid State Phys.* **1979**, *12*, 4827.
(28) Ridley, B. *J. Phys. C: Solid State Phys.* **1978**, *11*, 2323.
(29) Ahuja, B. L.; Jain, P.; Sahariya, J.; Heda, N. L.; Soni, P. *J. Phys. Chem. A* **2013**, *117* (27), 5685−5692.

DOI: 10.1021/acs.nanolett.5b02557
Nano Lett. 2015, 15, 5658−5663